

# The effect of focusing on polarization qubits

Netanel H. Lindner<sup>1,\*</sup> and Daniel R. Terno<sup>2,†</sup>

<sup>1</sup>*Department of Physics, Technion — Israel Institute of Technology, Haifa 32000, Israel*

<sup>2</sup>*Perimeter Institute for Theoretical Physics, Waterloo N2J 2W9, Ontario, Canada*

When a photon with well-defined polarization and momentum passes through a focusing device, these properties are no longer well defined. Their loss is captured by describing polarization by a  $3 \times 3$  effective density matrix. Here we show that the effective density matrix corresponds to the actual photodetection model and we provide a simple formula to calculate it in terms of classical fields. Moreover, we explore several possible experimental consequences of the “longitudinal” term: limits on single-photon detection efficiency, polarization-dependent atomic transitions rates and the implications on quantum information processing.

PACS numbers: 42.50.Dv, 03.67.Hk, 42.15.Dp

## I. INTRODUCTION

Single-photon manipulations have recently become an integral part of quantum optics and they play an important role in experimental quantum information processing [1]. Already with current technology the single-photon states can be produced and manipulated quite reliably [2], and the efficiency of their production and detection is expected to rise in the future. Usually these states are considered to be eigenstates of momentum, and often the very notion of photon is synonymous with an elementary excitation of the electromagnetic field with a well-defined momentum and polarization. A single-photon state  $|\mathbf{k}, \sigma\rangle = \hat{a}_{\mathbf{k}\sigma}^\dagger |\text{vac}\rangle$  is an excitation of the plane wave mode of momentum  $\mathbf{k}$  and polarization  $\sigma$  and is distributed over the entire space. An approximately localized photon [3] is described instead by a superposition

$$|\Psi\rangle = \int d\mu(\mathbf{k}) \sum_{\sigma} f_{\sigma}(\mathbf{k}) |\mathbf{k}, \sigma\rangle, \quad (1)$$

where  $\sigma$  denotes the helicity, the normalization is given by  $\sum_{\sigma} \int d\mu(k) |f_{\sigma}(\mathbf{k})|^2 = 1$ , while we adopt a non-relativistic measure  $d\mu(\mathbf{k}) = d^3\mathbf{k}/(2\pi)^3$ . More generally, localized states may be described as mixtures of such terms.

A typical spread in momentum is often very small, and polarization is approximately constant. As a result, polarization is usually described by a  $2 \times 2$  reduced density matrix which is formally equivalent to that of a qubit, the ideal unit of quantum information [4]. To ensure validity of this approximation and to calculate possible corrections, a general notion of polarization density matrix is required. However, the standard definition of reduced density matrix fails for photon polarization [5], and it is possible to define only an effective  $3 \times 3$  density matrix which corresponds to a restricted class of positive

operator-valued measures [6, 7]. Both experimental results and theoretical calculations for classical fields and for quantum coherent states [8, 9, 10] establish new effects that follow from the presence of a significant longitudinal electric field. This is often created by using focusing devices, which are also an inevitable part of usual optical experiments.

In this paper we apply the effective density matrix formalism to quantum states that correspond to classical modes with a significant longitudinal component and discuss its connection with experiment. The paper is organized as follows. Sec. II reviews effective  $3 \times 3$  density matrices and describes some of their applications. Sec. III presents a general formula that expresses an effective density matrix in terms of classical modes. It is illustrated by an elementary discussion of the lens action on one-photon states. Sec. IV discusses a connection between the formal construction of effective density matrix and a simple photodetection model. Finally, Sec. V introduces possible experimental consequences of the “longitudinal” term in effective density matrices.

## II. EFFECTIVE DENSITY MATRIX AND ITS APPLICATIONS

If one is interested only in polarization degrees of freedom, it is tempting to define a reduced  $2 \times 2$  density matrix by

$$\rho_{\sigma, \sigma'} = \int d\mu(\mathbf{k}) f_{\sigma}(k) f_{\sigma'}^*(k). \quad (2)$$

However, helicity eigenstates are defined only with respect to a given momentum. Intuitively, the polarization vectors for different momenta lie in different planes and cannot be superimposed. Under rotations each component acquires a momentum-dependent phase and hence the density matrix (2) has no definite transformation properties [5, 7]. This makes a standard density matrix a useless concept even when a fixed reference frame is considered, since any POVM (positive operator-valued measure [4, 11]) that describes an experimental setup must

\*Electronic address: lindner@technion.technion.ac.il

†Electronic address: dterno@perimeterinstitute.ca

have definite transformation properties at least under ordinary rotations. Analysis of the one-photon scattering [12] gives another angle on the failure of this concept.

The  $3 \times 3$  matrix with the right transformation properties may be introduced with the help of polarization 3-vectors [7]. A polarization state  $|\alpha(\mathbf{k})\rangle$  corresponds to the geometrical 3-vector

$$\alpha(\mathbf{k}) = \alpha_+(\mathbf{k})\epsilon_{\mathbf{k}}^+ + \alpha_-(\mathbf{k})\epsilon_{\mathbf{k}}^-, \quad (3)$$

where  $|\alpha_+|^2 + |\alpha_-|^2 = 1$ , and the vectors  $\epsilon_{\mathbf{k}}^\pm$  correspond to the right and left circular polarization and satisfy  $\mathbf{k} \cdot \epsilon_{\mathbf{k}}^\pm = 0$ . In this notation a generic one-photon state can be written as

$$|\Psi\rangle = \int d\mu(\mathbf{k}) f(\mathbf{k}) |\mathbf{k}, \alpha(\mathbf{k})\rangle, \quad (4)$$

and the effective  $3 \times 3$  description takes the form

$$\rho_{mn} = \int d\mu(\mathbf{k}) |f(\mathbf{k})|^2 \alpha_m(\mathbf{k}) \alpha_n(\mathbf{k})^*, \quad (5)$$

where  $m, n = x, y, z$  and the vector  $\alpha(\mathbf{k})$  is given by Eq. (3). Under rotations of the coordinate system this density matrix has a simple transformation law,

$$\rho \rightarrow R \rho R^T, \quad (6)$$

where  $R$  is the rotation matrix. The effective density matrix  $\rho$  can be obtained with the standard state-reconstruction techniques from a family of POVMs [6]. For example, its diagonal elements  $\rho_{ii}$  are the expectation values of the elements of the ‘‘momentum-independent’’ polarization POVM that consists of three positive operators  $E_i$  that sum up to the identity,  $\sum_i E_i = \mathbb{1}$ ,

$$\rho_{ii} = \langle \Psi | E_i | \Psi \rangle. \quad (7)$$

We discuss a relation between this POVM and the standard photodetection model in Sec. IV.

Let us now examine a wave packet which describes a nearly plane and nearly monochromatic wave. In this limit,  $f(\mathbf{k})$  of Eq. (4) is strongly localized around some central value  $\mathbf{k}_0$ . By an appropriate transformation of the form (6) the effective  $3 \times 3$  reduced density matrix can be put into a block diagonal form. Then the density matrix will have a  $2 \times 2$  block with almost unit trace, which corresponds to the standard  $2 \times 2$  reduced density matrix that would describe the state for  $f(\mathbf{k}) \propto \delta(\mathbf{k} - \mathbf{k}_0)$ . As an example, consider the following wavepackets that are formed by the helicity eigenstates,

$$|\Psi_\pm\rangle = \int d\mu(\mathbf{k}) f(\mathbf{k}) |\mathbf{k}, \epsilon_{\mathbf{k}}^\pm\rangle, \quad (8)$$

where  $f(\mathbf{k})$  satisfies the above criteria. Calculating the effective reduced density matrix we have

$$\rho_+ = \frac{1}{2}(1 - \frac{1}{2}\Omega^2) \begin{pmatrix} 1 & -i & 0 \\ i & 1 & 0 \\ 0 & 0 & 0 \end{pmatrix} + \frac{1}{2}\Omega^2 \begin{pmatrix} 0 & 0 & 0 \\ 0 & 0 & 0 \\ 0 & 0 & 1 \end{pmatrix}, \quad (9)$$

where  $\Omega \ll 1$  is roughly the ratio of a typical width of the wave packet to  $|\mathbf{k}_0|$ , and  $\rho_- = \rho_+^*$ . Its exact form depends on the detailed shape of  $f(\mathbf{k})$ . Thus we arrive to the conclusion that integrating out the photon’s momentum leads to polarization states that are neither pure nor perfectly distinguishable [5]. There is a non-zero probability to identify a  $\rho_+$  state as a  $\rho_-$  state and vice versa. The probability of making such an error given a perfect equipment and measurement scheme [13] will be denoted by  $P_E$  and is given by [7]

$$P_E(\rho_+, \rho_-) = \frac{1}{2} - \frac{1}{4} \text{tr} |\rho_+ - \rho_-| \approx \frac{1}{2} \Omega^2 \quad (10)$$

Although conceptually the implications of the above conclusions are profound, when considering a wave packet with a very narrow distribution in momentum  $f(\mathbf{k})$ , the parameter  $\Omega$  is very small. Consider an electromagnetic beam propagating along the  $z$ -axis and with the Gaussian distribution in intensity in the  $(xy)$  plane that is given by  $I(r) = I_0 \exp(-r^2/\tau^2)$ . Since the distribution in momentum  $f(\mathbf{k})$  is essentially the Fourier transform of the electric field, we expect that the radial spread in momentum will also be of the Gaussian form  $f(\mathbf{k}) \propto f_1(k_z) \exp(-k_r^2/2\Delta_r^2)$  where  $\Delta_r \sim 1/\tau$ , and  $f_1$  is some function of  $k_z$ . Assuming also the Gaussian distribution in wavelength  $f_1(k_z) \sim \exp(-(k_z - k_0)^2/2\Delta_z^2)$  we have

$$f(\mathbf{k}) = N \exp(-(k_z - k_0)^2/2\Delta_z^2) \exp(-k_r^2/2\Delta_r^2). \quad (11)$$

For this distribution in momentum, the parameter  $\Omega$  is given by [5]  $\Omega = \Delta_r/k_0 + O(\Delta_r^2/k_0^2)$ . Taking  $\tau$  to be of the orders of  $10^{-3}\text{m}$ , and a wavelength of  $5 \times 10^{-7}\text{m}$ , we get  $\Omega \sim 5 \times 10^{-4}$ , thus rendering the effect negligible.

However, the momentum spread becomes substantial when a beam undergoes focusing. A classical electromagnetic plane wave that passes through a converging lens is no longer plane or transversal [8, 9]. A substantial longitudinal field component is present as well as the effect described above.

### III. THE EFFECTS OF FOCUSING

In the analysis of the influence of a lens on quantum states it is important to bear in mind that it is incapable of turning a pure state into a mixture unless information is lost. Indeed, pure incoming state  $|\Psi_{\text{in}}\rangle$  transforms into a pure outgoing state  $|\Psi_{\text{out}}\rangle$ . The same information is encoded differently in these two states, and the effective density matrix captures our inability to access all of it. The lens action is analyzed by mode matching. To achieve this, we find a mode decomposition of solutions of the corresponding classical equation (in the case of photons these are the electromagnetic wave equations for the vector potential. Throughout this paper we use the Coulomb gauge). With each mode  $\mathbf{A}_{\mathbf{k}} = (2\pi)^{\frac{3}{2}} \epsilon_{\mathbf{k}}^\pm e^{-i(\omega t - \mathbf{k} \cdot \mathbf{x})}$  a creation operator  $\hat{a}_{\mathbf{k}\pm}^\dagger$  is associated. The resulting quantum state  $|\mathbf{k}, \pm\rangle = \hat{a}_{\mathbf{k}\pm}^\dagger |\text{vac}\rangle$

is normalized as  $\langle \mathbf{k}'\sigma' | \mathbf{k}, \sigma \rangle = \delta^{(3)}(\mathbf{k} - \mathbf{k}')\delta_{\sigma\sigma'}$ . All classical solutions are of the form

$$\mathbf{A}(t, \mathbf{x}) = A(t, \mathbf{x})\boldsymbol{\alpha}(t, \mathbf{x}) = \int d\mu(\mathbf{k})\boldsymbol{\alpha}(\mathbf{k})A(\mathbf{k})e^{-i(\omega t - \mathbf{k}\cdot\mathbf{x})}, \quad (12)$$

with  $\mathbf{E} = -\dot{\mathbf{A}}$ . The frequency  $\omega = |\mathbf{k}|c$ , each field component is split into the field strength  $A(\mathbf{k})$  and the transversal polarization part  $\boldsymbol{\alpha}(\mathbf{k})$ ,  $\mathbf{k}\cdot\boldsymbol{\alpha}(\mathbf{k}) = 0$ ,  $|\boldsymbol{\alpha}(\mathbf{k})| = 1$ . The corresponding norm is

$$\|\mathbf{A}\| = \|A\| = \left( \int d\mu(\mathbf{k})|A(\mathbf{k})|^2 \right)^{\frac{1}{2}}. \quad (13)$$

Therefore, a normalized positive energy solution of the form (12) corresponds to a one-particle state

$$\begin{aligned} |\Psi\rangle &= \sum_{\sigma=\pm} \int d\mu(\mathbf{k})\alpha_{\sigma}(\mathbf{k})f(\mathbf{k})\hat{a}_{\mathbf{k}\sigma}^{\dagger}|\text{vac}\rangle \\ &= \int d\mu(\mathbf{k})f(\mathbf{k})|\mathbf{k}, \boldsymbol{\alpha}(\mathbf{k})\rangle, \end{aligned} \quad (14)$$

where the coefficients  $\alpha_{\sigma}$  are defined by Eq. (3), and  $f(\mathbf{k}) = A(\mathbf{k})/\|A\|$ . The transformation  $|\Psi_{\text{in}}\rangle \rightarrow |\Psi_{\text{out}}\rangle$  is obtained from the transformation of the incoming modes  $\mathbf{A}_{\mathbf{k}}^{\text{in}}$  into the outgoing modes  $\mathbf{A}_{\mathbf{k}}^{\text{out}}$  [3, 14]. When the classical solution corresponding to the quantum state is known, the effective polarization density matrix Eq. (5) can be calculated as follows. We note that

$$\int A_n(\mathbf{x}, t)A_m^*(\mathbf{x}, t)d^3\mathbf{x} = \int A_n(\mathbf{k})A_m^*(\mathbf{k})d\mu(\mathbf{k}), \quad (15)$$

for all  $t$  and  $n, m = x, y, z$ . The density matrix (5), thus, can be written as

$$\rho = \frac{\int d\mu(\mathbf{k})\mathbf{A}(\mathbf{k})\mathbf{A}^{\dagger}(\mathbf{k})}{\int d\mu(\mathbf{k})|A(\mathbf{k})|^2}. \quad (16)$$

We stress that this is a general expression independent of approximations that are generally used to calculate classical solutions.

The analysis of the lens action should be performed in the vector diffraction theory [15], and reliable estimates of a field in the focal regions follow the techniques of Richards and Wolf [16]. In some cases it is even possible to get exact solutions of Maxwell equations [9]. Then, using Eq. (16) we find the outgoing quantum state whose effective reduced density matrix is calculated according to Eq. (5).

To illustrate the importance of the longitudinal term, it is sufficient to consider an incoming state with a definite momentum and polarization  $|\mathbf{k}, \boldsymbol{\epsilon}_{\mathbf{k}}^{\pm}\rangle$ , i.e. to approximate the corresponding classical field by a plane monochromatic wave. As we showed above, this is a good approximation for incoming wavepackets that are the actually used in experiments. Moreover, it is sufficient to use ray tracing, while more refined calculations should be used in conjunction with concrete experimental schemes. Hence

we take the outgoing classical field as a spherical wave that converges to the geometric focus of a thin lens with the focal length  $f$ , as illustrated on Fig. 1. The polarization direction and the field strength at each point are calculated using the eikonal equation and ray tracing [15].

The set-up is schematically presented on Fig. 1, while calculations are given in Appendix A. For the incoming states  $|\mathbf{k}, \boldsymbol{\epsilon}_{\mathbf{k}}^{\pm}\rangle$ , in the leading order the outgoing states are

$$\rho_{\pm} \approx (1 - \theta_m^2/4) \begin{pmatrix} \frac{1}{2} & \mp \frac{i}{4} & 0 \\ \pm \frac{i}{4} & \frac{1}{2} & 0 \\ 0 & 0 & 0 \end{pmatrix} + \theta_m^2/4 \begin{pmatrix} 0 & 0 & 0 \\ 0 & 0 & 0 \\ 0 & 0 & 1 \end{pmatrix}, \quad (17)$$

This is the only approximation which is consistent with

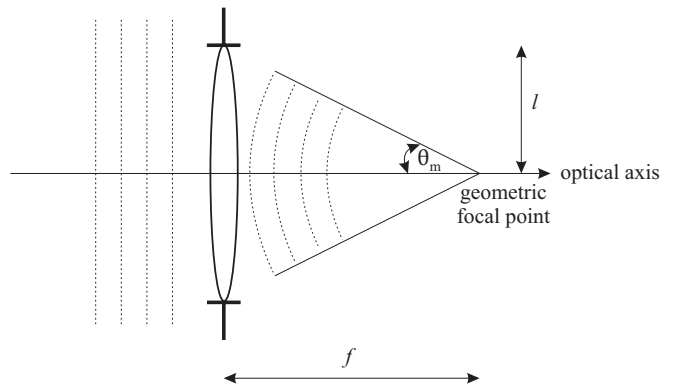


FIG. 1: Transformation of an incoming plane wave into a spherical wave by the focusing system.

use of Gaussian optics for mode calculation. All three eigenvectors are non-zero (even if, of course, the one that is associated with an ideal circular polarization dominates). The probability of error in distinguishing between  $\rho_+$  and  $\rho_-$  is proportional to the square of the numerical aperture,

$$P_E(\rho_+, \rho_-) = \frac{\theta_m^2}{8}. \quad (18)$$

Since  $\theta_m \approx l/f$  where  $l$  is the aperture radius, for the moderate numerical aperture of the order of  $10^{-1}$ , the probability of error gets to the level of percents, compared with a case with no lens present. The effects of “longitudinal” polarization will be even more pronounced when quantum states that correspond to classical doughnut-shaped [8] and other exotic modes are produced. This will be enhanced by going to higher numerical aperture, where the longitudinal field can contain nearly 50% of the total beam power in the limit  $\text{NA} \rightarrow 1$ .

#### IV. MEANING OF $\rho$

While the POVMs that were described in [6] are legitimate theoretical constructions, the resulting  $3 \times 3$  table becomes experimentally relevant if the POVM corre-

sponds to some detection model. We establish this correspondence. Let us compare predictions of the POVM  $E_x, E_y, E_z, \sum E_j = \mathbb{1}$  that gives the diagonal elements of the effective density matrix  $\rho_{jj} = \text{tr}(E_j|\Phi\rangle\langle\Phi|)$  [6, 7] with the detection probabilities that can be obtained from the first-order perturbational calculations of the following model detector. The operators  $E_j$  are given explicitly in Appendix B.

To facilitate the comparison we use an alternative form of the diagonal elements of the density matrix as in Eq. (16),

$$\rho_{jj} = W_j/W, \quad j = x, y, z, \quad (19)$$

where

$$W_j = \int |\mathbf{A} \cdot \hat{\mathbf{j}}|^2 dx dy dz, \quad W = \sum W_j. \quad (20)$$

We discuss here semiclassical detection theory, since in the leading order the results of the full theory agree with the semiclassical one [3]. In the latter the electromagnetic field is considered classically, while the photoelectrons are treated quantum-mechanically. The interaction term is given by  $\mathbf{p} \cdot \mathbf{A}$ , where  $\mathbf{A}$  is a classical vector potential (whose direction in the polarization gauge is given by the polarization vector  $\boldsymbol{\alpha}$ ) and  $\mathbf{p}$  is the electron's momentum operator. Accordingly, in the following we use a classical language to describe the electromagnetic field. The area  $S$  of a planar detector is assumed to be much larger than the cross section of the beam. We model the detector's sensitivity to the wave's polarization by restricting the electron momentum to lie only along a chosen direction.

Let us first consider a circularly polarized monochromatic beam in the paraxial approximation [17]. Assuming that it propagates along the  $z$ -axis, we have

$$\mathbf{E}(\mathbf{x}, t) \approx \left( E(x, y) \boldsymbol{\epsilon}^\pm + \frac{i}{k} \left( \frac{\partial E}{\partial x} \pm i \frac{\partial E}{\partial y} \right) \hat{\mathbf{z}} \right) e^{-i(\omega_0 t - k_0 z)}, \quad (21)$$

$$\mathbf{B} \approx \mp i \mathbf{E}, \quad (22)$$

where the basis polarization vectors are  $\boldsymbol{\epsilon}^\pm = \sqrt{\frac{1}{2}}(1, \pm i, 0)$  and the beam radius  $\tau$  is much larger than a typical wavelength,  $\tau k_0 \gg 1$ .

Let the planar detector absorb the field along the  $j$ -axis ( $j = x, y, z$ ) and locate it at  $z = z_0$ . Hence, electrons' excitation rate is proportional to  $\int |\mathbf{A}(x, y, z_0) \cdot \hat{\mathbf{j}}|^2 dS$ . Assuming a finite detection time  $\Delta$  (or a beam of finite duration  $\Delta$ , with the fields that are given by the corresponding superpositions of  $\mathbf{E}$  and  $\mathbf{B}$  having different frequencies with some weight function  $f = f(\omega - \omega_0)$ ), the excitation probability is proportional to

$$I_j = \int |\mathbf{A}(x, y, z_0) \cdot \hat{\mathbf{j}}|^2 dS dt. \quad (23)$$

Since the detector is planar, we can change the integration variable from  $t$  to  $z$  we get

$$I_j = \Delta \int |\mathbf{A}(x, y, z_0) \cdot \hat{\mathbf{j}}|^2 dx dy \quad (24)$$

$$= \int_{x, y} \int_{z=z_0-\Delta c}^{z=z_0} |\mathbf{A}(x, y, z) \cdot \hat{\mathbf{j}}|^2 dx dy dz. \quad (25)$$

Hence  $I_j = W_j$ , and the diagonal elements of  $\rho$  are indeed related to the photocurrent as

$$\rho_{ss} = I_j/I, \quad I = \sum I_j. \quad (26)$$

Now consider a spherical wave which represents the EM field after the lens, as in Eqs. (34)-(36),(41). We again consider a planar wave detector and detection time  $\Delta$ . This time, however, the normal to the detector plane is not parallel to the Pointing vector, and thus  $I_j/I$  are different from  $W_j/W$ . Nevertheless, as will be seen shortly, these ratios agree up to the order  $\theta_m^4$ , while for the realistic values of  $\theta_m$  the interesting effects (such as the predicted error probability, Eq. (18)) are of the order  $\theta_m^2$ .

Let us assume that the detector is located at  $z = z_0$  behind the focus. We use spherical coordinates with the origin in the focus and  $\theta = 0$  at  $z = z_0$ , and polar coordinates in the detector plane. In this plane  $\phi$  is the same as in the spherical coordinates and  $r = z_0 \tan \theta$ . From the result of Appendix A, the field strength  $E$  can be written as

$$E = E(R, \theta) = \frac{1}{(\cos \theta)^{3/2}} \frac{1}{r} = \frac{e(\theta)}{r}, \quad (27)$$

and since we are working with a well defined frequency, a similar decomposition is possible for  $A$ , i.e.,  $A = a(\theta)/r$ . The point  $(\theta, \phi)$  on the detector plane is at a distance  $z_0/\cos \theta$  from the focus. The area element is

$$dS = \frac{\sin \theta}{\cos^3 \theta} z_0^2 d\theta d\phi, \quad (28)$$

so the detection probability is proportional to

$$I_j = \Delta \int |a(\theta)|^2 |\boldsymbol{\alpha}(\theta, \phi) \cdot \hat{\mathbf{j}}|^2 \tan \theta d\theta d\phi. \quad (29)$$

On the other hand, the integration over the shell  $\Delta c$  gives

$$W_j = \Delta \int |a(\theta)|^2 |\boldsymbol{\alpha}(\theta, \phi) \cdot \hat{\mathbf{j}}|^2 \sin \theta d\theta d\phi. \quad (30)$$

The normalized detection probabilities

$$p_j = I_j/I, \quad (31)$$

differ therefore from the matrix elements of  $\rho_{jj} = W_j/W$  by the presence of additional factors  $1/\cos \theta$  in each of the integrals. However, when the results are expanded in terms of  $\theta_m$ , the difference between these two expressions

is only of the order of  $\theta_m^4$  or higher. Accordingly, the leading order expansion for the probability of error, Eq. (18), remains the same for the model detection scheme that was described above. This discrepancy highlights the fact that *different detection procedures lead to different polarization density matrices* [12]. Moreover, with a slight abuse of the language, we note that the resulting effective mixing is caused by the shape mismatch between the wave front and the detector.

## V. SUMMARY AND OUTLOOK

We have shown that an effective  $3 \times 3$  polarization density matrix, previously introduced on formal grounds, indeed has a direct experimental significance. It should be noted, however, since there is no general polarization density matrix, different detection procedures may lead to different effective constructions.

Presence of a significant longitudinal part in the effective density matrix imposes limits on detection efficiency. The interaction between single atoms and electromagnetic field, either classical or in a quantum coherent state, is affected by focusing [9, 10]. The structure of the effective density matrix shows that this will be the case also for single photon states. Polarization-sensitive transitions in the atoms will be suppressed by strong focusing. For low numerical apertures we expect these effects to be proportional to its square, reaching saturation on higher levels when  $NA \rightarrow 1$ . From the point of view of quantum information theory, the fact that these density matrices are inevitably mixed, actually implies that polarization qubits are always noisy. This intrinsic noise should be taken into account in the analysis of the physical realizations of quantum computing and in the security analysis of quantum cryptographic protocols. Similarly, sensitivity of photon-atom interaction to the focusing will affect the efficiency of trapped-atom based quantum memory [1].

### Acknowledgments

The work of NHL is supported by a grant from the Technion Graduate School. Parts of this research were done during the visit of NHL to the Perimeter Institute and of DRT to the University of Queensland. The importance of focusing effects was pointed out to us by Eli Yablonovich. We thank Gerard Milburn, Petra Scudo, Christine Silberhorn, Vlatko Vedral and Andrew White for useful discussions and helpful comments.

### APPENDIX A

Assume that the optical axis is the  $z$ -axis, and approximate the incoming classical wave as a plane wave with

$\hat{\mathbf{k}} = \hat{\mathbf{z}}$  and polarization  $\boldsymbol{\alpha}$ . Two systems of coordinates will be used in the following. The plane  $z = 0$  is the plane where the lens is situated. In it we define polar coordinates  $(r, \phi)$ , where  $r$  is measured from the optical axis in the  $z = 0$  plane. The unit vectors  $\hat{\mathbf{r}}, \hat{\phi}$  will always lie in the  $z = 0$  plane. The spherical coordinates  $(R, \theta, \phi)$  are calculated from the focus (the angles  $\phi$  in both coordinate systems are the same). The intersection between the optical axis and  $z = 0$  plane has  $r = f$  and  $\theta = 0$  coordinates, while the lens aperture is bounded by  $\theta_m$ . The relation

$$r = f \tan \theta, \quad (32)$$

holds on the plane  $z = 0$ , while  $\theta_m$ ,

$$\tan \theta_m = l/f, \quad (33)$$

is determined by the nominal focal ratio [15]  $F = f/2l$ , where  $l$  is the radius of the entrance pupil. In the Gaussian approximation  $\theta_m$  equals to the numerical aperture. Assuming that after passing through the lens the field

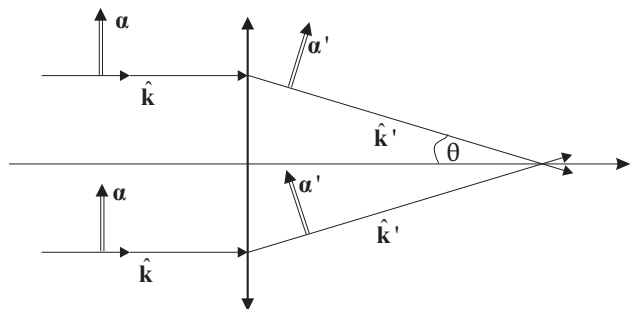


FIG. 2: Changes in a linear polarization according to the ray-tracing model. The direction and polarization labels  $\hat{\mathbf{k}}$  and  $\boldsymbol{\alpha}$  of the ray are transformed into  $\hat{\mathbf{k}}'(\theta, \phi)$  and  $\boldsymbol{\alpha}'(\theta, \phi)$ , respectively.

is that of a perfect spherical wave, the ray that hits the  $z = 0$  plane at  $(r, \phi)$  is deflected to the direction

$$\hat{\mathbf{k}}'(\theta) = -\sin \theta \hat{\mathbf{r}} + \cos \theta \hat{\mathbf{z}} = -\sin \theta (\cos \phi \hat{\mathbf{x}} + \sin \phi \hat{\mathbf{y}}) + \cos \theta \hat{\mathbf{z}}, \quad (34)$$

with  $\theta$  given by Eq. (32). In passing through a homogeneous dielectric medium polarization directions are parallel transported along each ray. At the boundaries the direction that is parallel to the incidence plane is refracted to remain transversal to the wave vector, while the perpendicular component is unchanged [15, 17]. The incidence plane is spanned by the vectors  $\hat{\mathbf{z}}$  and  $\hat{\mathbf{r}}$ , so that the parallel and perpendicular components of polarization are  $\hat{\mathbf{r}}$  and  $\hat{\phi}$ , respectively. We decompose the polarization of the ray that passes through the  $z = 0$  plane at  $(r, \phi)$ , in terms of  $\hat{\mathbf{r}}$  and  $\hat{\phi}$ . For linear  $x$ -polarization it is given by

$$\boldsymbol{\alpha}_x \equiv \hat{\mathbf{x}} = \cos \phi \hat{\mathbf{r}} - \sin \phi \hat{\phi}. \quad (35)$$

Having passed through the  $z = 0$  plane, the new direction of polarization for the above ray becomes

$$\boldsymbol{\alpha}'_x(\theta, \phi) = \cos \phi (\cos \theta \hat{\mathbf{r}} + \sin \theta \hat{\mathbf{z}}) - \sin \phi \hat{\boldsymbol{\phi}}, \quad (36)$$

were again  $\theta$  is related to  $r$  by Eq. (32). The same calculation can be carried out for the linear  $y$  polarization, giving

$$\boldsymbol{\alpha}'_y(\theta, \phi) = \sin \phi (\cos \theta \hat{\mathbf{r}} + \sin \theta \hat{\mathbf{z}}) + \cos \phi \hat{\boldsymbol{\phi}}. \quad (37)$$

It is easy to see that right and left circular polarizations are preserved up to a phase,  $\boldsymbol{\epsilon}_{\mathbf{k}}^{\pm} \rightarrow e^{\pm g(\theta, \phi)} \boldsymbol{\epsilon}_{\mathbf{k}'}^{\pm}$ , where the precise form of  $g$  is irrelevant. Fig. 2 illustrates these changes.

To complete the classical description of the field as in Eq. (12), we need the field strength  $E(\mathbf{k})$ . Calculations of the intensity are based on the intensity law of geometrical optics [15],

$$E^2 dS = E'^2 dS', \quad (38)$$

where  $E$ ,  $dS$  and  $E'$ ,  $dS'$  are the field strength and the area element at the respective wavefronts. Taking the initial field strength to be unity, and considering that the wavefronts before the lens are planar,

$$dS = 2\pi r(\theta) dr(\theta) = 2\pi \frac{\sin \theta}{\cos^3 \theta} f^2 d\theta, \quad (39)$$

and that after the lens they are spherical,

$$dS' = 2\pi \sin \theta R^2 d\theta, \quad (40)$$

we get

$$E'(R, \theta) = \frac{1}{(\cos \theta)^{3/2}} \frac{f}{r}. \quad (41)$$

Since both the plane wave and the spherical wave are non-normalizable, we obtain the density matrices from the two-dimensional integration over the angular parts of the volume integral. For the incoming states  $|\mathbf{k}, \boldsymbol{\epsilon}_{\mathbf{k}}^{\pm}\rangle$ , taking into account that  $\omega = |\mathbf{k}'|c = \text{const}$ , the outgoing states are

$$\rho = \frac{\int_{\psi=0}^{2\pi} \int_{\theta=0}^{\theta_m} \sin \theta d\theta d\psi \boldsymbol{\epsilon}_{\pm}(\theta, \psi) \boldsymbol{\epsilon}_{\pm}^{\dagger}(\theta, \psi) / \cos^3 \theta}{\int d\theta d\psi \sin \theta / \cos^3 \theta}, \quad (42)$$

whose explicit form is given by Eq. (17).

## APPENDIX B

The required POVM is introduced as follows. The longitudinal photons are used to define the necessary steps

of our construction. The POVM itself is build only with the physical polarization states. Allowing for longitudinal polarization makes it possible to define a polarization state along an arbitrary direction, say the  $x$ -axis, as

$$|\hat{\mathbf{x}}\rangle = x_+(\mathbf{k})|\boldsymbol{\epsilon}_{\mathbf{k}}^+\rangle + x_-(\mathbf{k})|\boldsymbol{\epsilon}_{\mathbf{k}}^-\rangle + x_\ell(\mathbf{k})|\boldsymbol{\epsilon}_{\mathbf{k}}^\ell\rangle, \quad (43)$$

where  $x_{\pm}(\mathbf{k}) = \boldsymbol{\epsilon}_{\mathbf{k}}^{\pm} \cdot \hat{\mathbf{x}}$ , and  $x_\ell(\mathbf{k}) = \hat{\mathbf{x}} \cdot \mathbf{k}$ . Note that  $\langle \hat{\mathbf{x}} | \hat{\mathbf{y}} \rangle = \hat{\mathbf{x}} \cdot \hat{\mathbf{y}} = 0$ , whence

$$|\hat{\mathbf{x}}\rangle \langle \hat{\mathbf{x}}| + |\hat{\mathbf{y}}\rangle \langle \hat{\mathbf{y}}| + |\hat{\mathbf{z}}\rangle \langle \hat{\mathbf{z}}| = \mathbb{1}. \quad (44)$$

A projection operator that corresponds to the direction  $\hat{\mathbf{x}}$  is

$$P_x = |\hat{\mathbf{x}}\rangle \langle \hat{\mathbf{x}}| \otimes \mathbb{1}_p = |\hat{\mathbf{x}}\rangle \langle \hat{\mathbf{x}}| \otimes \int d\mu(\mathbf{k}) |\mathbf{k}\rangle \langle \mathbf{k}|, \quad (45)$$

where  $\mathbb{1}_p$  is the unit operator in momentum space. The action of  $P_x$  on a physical state  $|\Psi\rangle$  follows from Eq. (43) and  $\langle \boldsymbol{\epsilon}_{\mathbf{k}}^{\pm} | \boldsymbol{\epsilon}_{\mathbf{k}}^\ell \rangle = 0$ . Only the transversal part of  $|\hat{\mathbf{x}}\rangle$  appears in the expectation value:

$$\langle \Psi | P_x | \Psi \rangle = \int d\mu(\mathbf{k}) |f(\mathbf{k})|^2 |x_+(\mathbf{k})\alpha_+(\mathbf{k}) + x_-(\mathbf{k})\alpha_-(\mathbf{k})|^2. \quad (46)$$

Define the transversal part of  $|\hat{\mathbf{x}}\rangle$ :

$$\begin{aligned} |\mathbf{k}, \mathbf{b}_x(\mathbf{k})\rangle &\equiv (|\boldsymbol{\epsilon}_{\mathbf{k}}^+\rangle \langle \boldsymbol{\epsilon}_{\mathbf{k}}^+| + |\boldsymbol{\epsilon}_{\mathbf{k}}^-\rangle \langle \boldsymbol{\epsilon}_{\mathbf{k}}^-|) |\hat{\mathbf{x}}\rangle \\ &= x_+(\mathbf{k})|\boldsymbol{\epsilon}_{\mathbf{k}}^+\rangle + x_-(\mathbf{k})|\boldsymbol{\epsilon}_{\mathbf{k}}^-\rangle, \end{aligned} \quad (47)$$

and likewise  $|\mathbf{b}_y(\mathbf{k})\rangle$  and  $|\mathbf{b}_z(\mathbf{k})\rangle$ . These three vectors are neither of unit length nor mutually orthogonal.

Finally, a POVM element  $E_x$  which is the physical part of  $P_x$ , namely is equivalent to  $P_x$  for physical states (without longitudinal photons) is

$$E_x = \int d\mu(\mathbf{k}) |\mathbf{k}, \mathbf{b}_x(\mathbf{k})\rangle \langle \mathbf{k}, \mathbf{b}_x(\mathbf{k})|, \quad (48)$$

and likewise for other directions. The operators  $E_x$ ,  $E_y$  and  $E_z$  indeed form a POVM in the space of physical states, owing to Eq. (44). It then follows from Eq. (47) and similar definitions for the other directions that, for any  $\mathbf{k}$ ,

$$|\mathbf{b}_x(\mathbf{k})\rangle \langle \mathbf{b}_x(\mathbf{k})| + |\mathbf{b}_y(\mathbf{k})\rangle \langle \mathbf{b}_y(\mathbf{k})| + |\mathbf{b}_z(\mathbf{k})\rangle \langle \mathbf{b}_z(\mathbf{k})| = \mathbb{1}_{\perp \mathbf{k}}, \quad (49)$$

where  $\mathbb{1}_{\perp \mathbf{k}}$  is the identity operator in the subspace of polarizations orthogonal to  $\mathbf{k}$ .

[1] D. Bouwmeester, A. K. Ekert, A. Zeilinger, *The Physics of Quantum Information: Quantum Cryptogra-*

*phy, Quantum Teleportation, Quantum Computation*; N.

- G. Gisin, G. Ribordy, W. Tittel, and H. Zbinden, *Rev. Mod. Phys.* **74**, 145 (2002).
- [2] J. Vučković, D. Fattal, C. Santori, G. S. Solomon, and Y. Yamamoto, *Appl. Phys. Lett.* **82**, 3596 (2003); A. B. U'Ren, Ch. Silberhorn, K. Banaszek, I. A. Walmsley, e-print quant-ph/0312118.
- [3] L. Mandel and E. Wolf, *Optical Coherence and Quantum Optics* (Cambridge University Press, Cambridge, 1995), ch. 6, 12.
- [4] A. Peres, *Quantum Theory: Concepts and Methods* (Kluwer, Dordrecht, 1993); M. A. Nielsen and I. L. Chuang, *Quantum Computation and Quantum Information* (Cambridge University Press, New York, 2000).
- [5] N. H. Lindner, A. Peres and D. R. Terno, *J. Phys. A* **36**, L449 (2003).
- [6] A. Peres and D. R. Terno, *J. Mod. Opt.* **50**, 1165 (2003).
- [7] A. Peres and D. R. Terno, *Rev. Mod. Phys.* **76**, 93 (2004).
- [8] R. Dorn, S. Quabis, G. Leuchs, *Phys. Rev. Lett.* **91**, 232901 (2003); R. Dorn, S. Quabis, G. Leuchs, *J. Mod. Opt.* **50**, 1917 (2003).
- [9] S. J. van Enk and H. J. Kimble, *Phys. Rev. A* **61**, 051802 (R) (2000); S. J. van Enk and H. J. Kimble, *Phys. Rev. A* **63**, 023809 (2001).
- [10] S. J. van Enk, e-print quant-ph/0307216.
- [11] P. Busch, M. Grabowski, and P. J. Lahti, *Operational Quantum Physics* (Springer, Berlin 1995).
- [12] A. Aiello and J. P. Woerdman, e-print quant-ph/0404029.
- [13] C. A. Fuchs and J. van de Graaf, *IEEE Trans. Info. Theory* **IT-45**, 1216 (1999).
- [14] M. O. Scully and M. S. Zubairy, *Quantum Optics* (Cambridge University Press, Cambridge, 1997).
- [15] M. Born and E. Wolf, *Principles of Optics* (Cambridge University Press, Cambridge, 1999), ch. III, IV.
- [16] B. Richards and E. Wolf, *Proc. Roy. Soc. London A* **253**, 359 (1959); J. Stannnes, *Waves in Focal Regions* (Adam Hilger, Bristol, 1986); S. Quabis, R. Dorn, M. Eberler, O. Glöckl, and G. Leuchs, *Appl. Phys. B* **72**, 109 (2001).
- [17] J.D. Jackson, *Classical Electrodynamics* (John Wiley & Sons, New York, 1975), ch. 7.